ELSEVIER

Biophysical Chemistry 107 (2004) 175–187

Biophysical Chemistry

www.elsevier.com/locate/bpc

Aggregation kinetics of bovine serum albumin studied by FTIR spectroscopy and light scattering

Valeria Militello*, Carlo Casarino, Antonio Emanuele, Antonella Giostra, Filippo Pullara, Maurizio Leone

INFM and Department of Physical and Astronomical Sciences, Università di Palermo, Via Archirafi 36, 90123 Palermo, Italy

Received 6 August 2003; received in revised form 12 September 2003; accepted 12 September 2003

Abstract

To investigate which type of structural and conformational changes is involved in the aggregation processes of bovine serum albumin (BSA), we have performed thermal aggregation kinetics in D_2O solutions of this protein. The tertiary conformational changes are followed by Amide II band, the secondary structural changes and the formation of β-aggregates by the Amide I′ band and, finally, the hydrodynamic radius of aggregates by dynamic light scattering. The results show, as a function of pD, that: tertiary conformational changes are more rapid as pD increases; the aggregation proceeds through formation of ordered aggregates (oligomers) at pD far from the isoelectric point of the protein; disordered structures add as the pD decreases. Moreover, β-aggregates seem to contribute only to oligomers formation, as showed by the good correlation between kinetics of scattering intensity and IR absorption intensity. These results indicate for BSA a general mechanism of aggregation composed by partial unfolding of the tertiary structure and by the decrease of α-helix and random coil contents in favor of β-sheet aggregates. This mechanism strictly depends on pD and gives rise to almost two distinct types of macromolecular aggregates.

Keywords: Bovine serum albumin; Protein aggregation; Infrared spectroscopy; Conformational changes; Static light scattering; Dynamic light scattering

1. Introduction

The relationship between the conformational and structural properties of proteins and the intermolecular interactions that give rise to the aggregation processes has been object, in the last years, of many biophysical and pharmaceutical studies [1–5]. In particular, studies on different proteins suggested a multistage aggregation mechanism in which partial unfolding of native protein was the initial step [6]. In thermally induced aggregation, the compact native form of protein, with its well-defined secondary and tertiary structures, becomes more flexible on heating and more reactive towards its neighbors. The degree to which it happens is temperature- and time-dependent, and is itself a multi-stages process [6]. Increasing the temperature, some molecular regions of proteins, like hydrophobic regions or free SH-groups, become

*Corresponding author. Tel.: +39-91-6234299; fax: +39-91-6162461.

E-mail address: militelo@fisica.unipa.it (V. Militello).

0301-4622/04/$ - see front matter © 2003 Elsevier B.V. All rights reserved.
doi:10.1016/j.bpc.2003.09.004

accessible to new intermolecular interactions, forming soluble aggregates through non-covalent and disulfide bonds [7,8]. Moreover, intermolecular β-sheet formation can take place and contribute to intermolecular association of the partially unfolded protein molecules [9]. All these intermolecular interactions can give origin to the protein gelling phenomenon [6] and can mainly be driven by surface net charge and hydrophobic area exposed to the solvent. In this sense, Park et al. have found that the structure of heat induced protein gel can be controlled by adjusting either surface net charge or hydrophobicity [10]. This has a relevant implication at pharmaceutical level because it is possible to design controlled structures of gels as drug carriers.

The aggregation process of proteins is strongly affected by temperature, time of heating, concentration and pH. For example, heating native serum albumin to approximately 80 °C causes reversible denaturation; whereas, heating for a longer period at 60 °C, causes irreversible denaturation [11–13]. In particular, when temperature increases, electrostatic interactions are not substantially modified, whereas, hydrophobic interactions are strengthened, due to their entropic origin [14]. Moreover, changes in pH lead to titration of groups in the unfolded form, causing destabilization of overall native protein structure [15] and strongly affecting the protein aggregation rate [7]. At extreme pH values, far from isoelectric point (p*I*), electrostatic repulsion between like charges in protein increases, resulting in a larger tendency to unfold, and modifies the intermolecular interactions [16–19]. Moreover, at a fixed temperature and pH values, the size of aggregates depends on concentration [20]; in particular, changing the concentration, it is possible to drive the aggregates formation from oligomers to gel [21,22].

In this scenario, many aspects concerning the correlation between the structural and conformational changes of protein and the degree and type of aggregation remain open questions. The experimental approach usually used to monitor these aspects is based on several spectroscopic techniques like CD, Raman, infrared spectroscopy and fluorescence [23–26].

We have already performed a study on temperature induced conformational changes of bovine serum albumin (BSA) at tertiary and secondary level followed by steady-state fluorescence and CD, to have information on preliminary steps of BSA aggregation processes in the low concentration regime [27].

In this work, we report a study on the effects of pD changes on aggregation kinetics of BSA to see if and how, in our conditions, intra- and intermolecular interactions can depend on surface net charge. The conformational changes at tertiary level are followed by the H–D exchange of the partially unfolded protein through time evolution of Amide II band. Besides, the structural changes at secondary level are followed by time evolution of Amide I′ band profile. This band is a probe of protein structural organization in terms of α-helix, random coil and β-sheet contents and gives information on protein–protein aggregation through the appearance of two shoulders attributed to β-sheet formation [9,28–33]. Finally, to have information on the mean dimensions of aggregates, dynamic light scattering measurements have also been performed.

2. Materials and methods

2.1. Sample preparation

BSA (type A-0281) was purchased from Sigma; D_2O was purchased from Eurisotop (99.97%). At each pD value, the relative phosphate buffer was prepared in H_2O and then diluted at 10% in D_2O, at a final concentration of 0.1 M. We note that pD values were corrected by 0.4 (i.e. pD = pH meter reading + 0.4) [32]. Samples, freshly prepared dissolving 60 mg ml^{-1} of BSA, centrifuged (2000 rpm) and passed through 0.22-μm filters, were divided in two aliquots for IR and light scattering measurements. Each sample was incubated at 58 °C and, for both experimental techniques, the time evolution of signals was followed; the time $t = 0$ was considered after 7 min by positioning protein sample in the thermostable sample compartment.

2.2. IR measurements

The single-beam IR spectra were measured using a BIO-RAD FTS-40A spectrometer equipped

with a PbS detector, with a spectral resolution of 1 cm^{-1} and 100 scans. All samples were placed between two CaF_2 windows, with a 0.025-mm Teflon spacer. In a separate experiment, the single-beam spectrum of each solvent was measured, at the same temperature. Sample and solvent absorption spectra were calculated with respect to the single-beam of empty cell. Finally, for each pD value, the relative solvent spectrum was subtracted to the sample one, after suitable normalization. D_2O solutions were used to avoid the spectral overlaps between Amide I band and strong ν_2 absorption band of water at approximately 1650 cm^{-1}, and to monitor the H–D exchanges between protein and solvent by Amide II. For clarity, here we recall the assignments of the observed bands. Amide I and Amide II bands of proteins in H_2O solutions are centered at approximately 1660 and 1550 cm^{-1}, respectively, and shift towards 1650 cm^{-1} (Amide I′) and 1450 cm^{-1} (Amide II′) in D_2O solutions [34,35]. Amide I is primarily attributed to an out-of-phase combination of C=O and C–N stretchings of amide groups. Generally, Amide I band has a composite band profile, consisting of several spectral components related to the different secondary structures [36–41]. Besides, Amide II band is attributed to an out-of-phase combination of in-plane C–N stretching and N–H bending of amide groups. We outline that all absorption bands are normalized for BSA concentration by diving for the absorption intensity at 1650 cm^{-1} of each sample, at room temperature.

2.3. Light scattering measurements

Light scattering measurements were performed on a Brookhaven goniometer BI-SM200, at fixed 90° scattering angle, using a BI-9000AT correlator and a duplicated Nd-doped solid state laser, $\lambda = 532$ nm. Both static (SLS) and dynamic (DLS) light scattering measurements were performed, with 100 s of integration time; the intensity correlation function is obtained by acquiring data between 5 and 1000 μs, in 200 channels. The intensity of scattered light (SLS measurements) allows us to obtain the amount of aggregates in the sample. From DLS measurements, the diffusion coefficient of particles in solution can be obtained, and, by the analysis of the intensity autocorrelation function delineate below, the radius of the particles in solution can be determined.

In the case of a solution of N different sized species, the autocorrelation function can be fitted by using the following equation [42]:

$$G_2(t) = \left[\sum_{j=1}^{N} c_j \exp(-a_j t)\right]^2 \quad (1)$$

where c_j is an amplitude factor proportional to the mean number of particles of a given radius and a_j is defined as $a_j = D_j q^2$, q being the scattering vector and D_j the diffusion coefficient. Making use of the Stoke–Einstein relation for D_j, we obtain the hydrodynamic radius of each specie of particles. In particular, for our measurements the analysis is made in terms of one or two species. In this last case, we can obtain the contributions of the two species, I_1 and I_2, to the total intensity, I, as:

$$I_{1,2} = I\frac{c_{1,2}}{c_1 + c_2}. \quad (2)$$

We have also made a parallel analysis of autocorrelation function by means of CONTIN method [43]. Using this analysis, we can obtain the fraction of light scattered by species having a determined value of the radius [44]. With CONTIN analysis, we can also obtain mean weighted-intensity radius of each specie. This radius coincides, in a satisfactory way, with the hydrodynamic radius obtained by single and double exponential decay analysis.

3. Results and discussion

Fig. 1 shows absorption spectra in the Amides region of a BSA sample in native (room temperature) and aggregated forms (after 2 h of incubation at 58 °C).

As can be seen, BSA exhibits an intense Amide I′ band centered at approximately 1650 cm^{-1}, in agreement with the reported percentage of α-helix structure in the native form (~66%) [45]; in the same region, spectral contributions at lower fre-

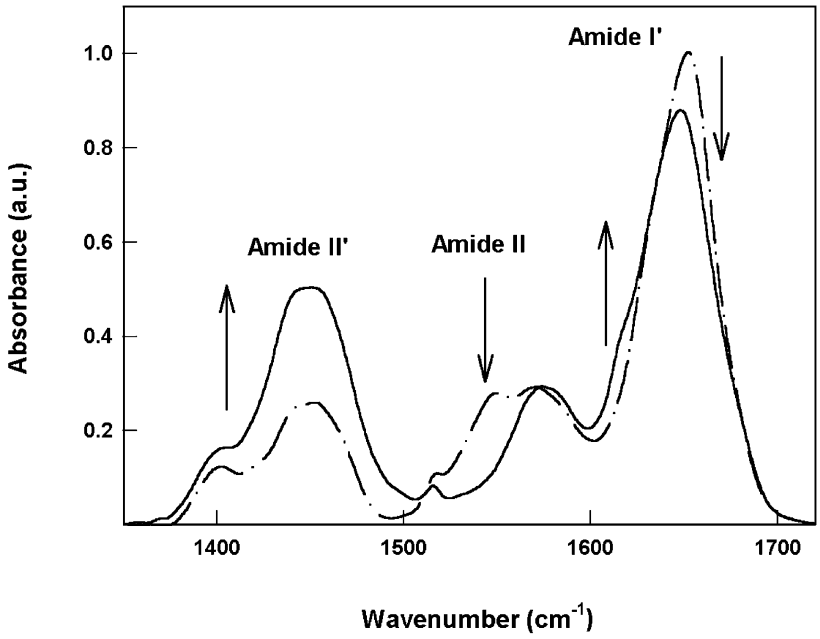

Fig. 1. IR absorption spectra of BSA at pD 7.4, at room temperature (native form, dashed–dotted line) and after 120 min of incubation at 58 °C (aggregated form, solid line). The arrows indicate the changes in the main Amide band profiles from native to aggregated form.

quencies can contribute to the overall band profile, typically attributed to random coil structures (~31% in the native form). We do not distinguish between these two spectral contributions so, in the following, we will consider mainly the larger one due to the α-helix structure. The intensity of this band decreases when protein is in the aggregated form, suggesting a partial loose of the α-helix content. Moreover, this decreasing is accompanied by the appearance of two shoulders at 1620 and 1680 cm^{-1}, that are attributed to the intermolecular β-sheet aggregates [9,28–33]. The formation of intermolecular strand structures in thermally induced protein aggregates was clearly demonstrated by Clark et al., by using small angle X-ray scattering [46,47]. In our sample, the presence after 2 h of incubation at 58 °C, of these two shoulders reveals the formation of these intermolecular β-sheet aggregates.

Moreover, as clearly shown in Fig. 1, both Amide II and Amide II′ spectral contributions are present and, in particular, before and after 2 h at 58 °C, one decreases and the other increases. This suggests that the hydrogens remained within the core of the protein, that are inaccessible to the solvent in the native form, can undergo to H–D exchange during the incubation time, as the protein partially unfolds. We have studied the kinetic of this exchange by following the time evolution of IR spectra in the Amide II region as a function of pD. As can be seen, in Fig. 2 the decrease of Amide II at approximately 1540 cm^{-1} and the increase of Amide II′ at approximately 1450 cm^{-1} are strictly related, suggesting that an exchange occur in our sample, indicative of a conformational changes at a tertiary structural levels. As reported in Fig. 3, at pD 7.4 this exchange stops after 20 min, while at lower pD it slows down until 50 min.

It is noteworthy that, by changing pD, different values are observed in the Amide II at the beginning of the kinetics, whereas the same value is obtained for times longer than 60 min. This could be due to small differences in the native tertiary

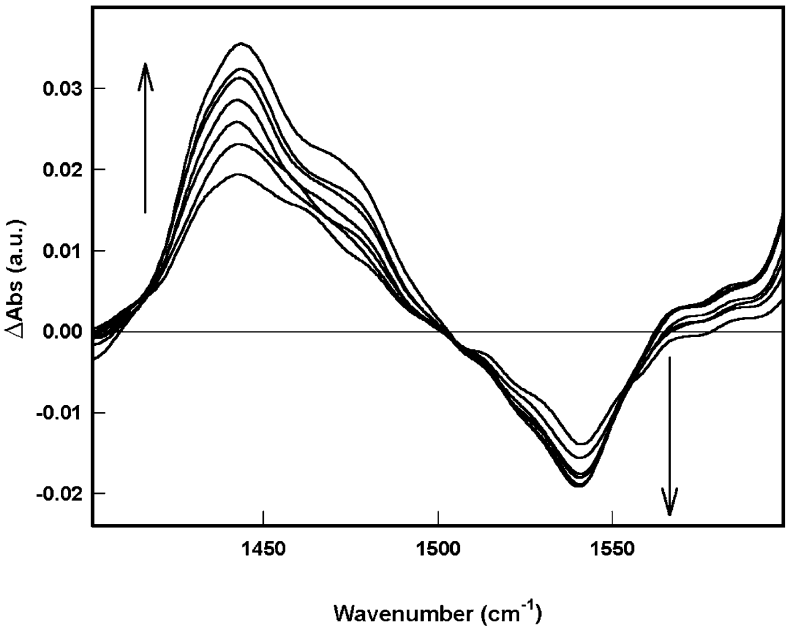

Fig. 2. Time evolution of differential spectra, defined as $\Delta A(t)=A(t)-A(t=0)$, in the Amide II region of BSA, at pD 7.4 and at 58 °C.

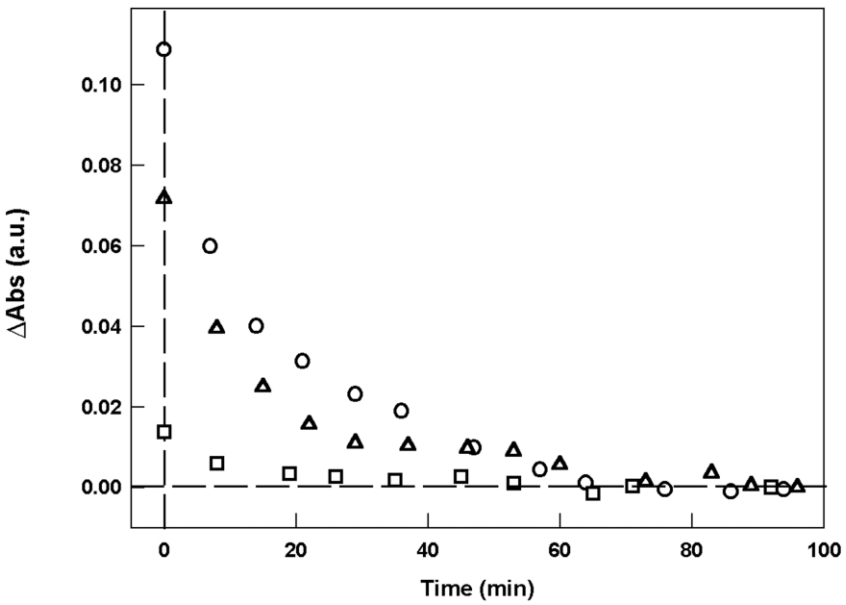

Fig. 3. Time evolution of differential absorption intensity, defined as $\Delta A(t)=A(t)-A(t=0)$, at 1540 cm^{-1} (Amide II) of BSA, at 58 °C. Squares: pD 7.4; triangles: pD 6.8; circles: pD 6.2.

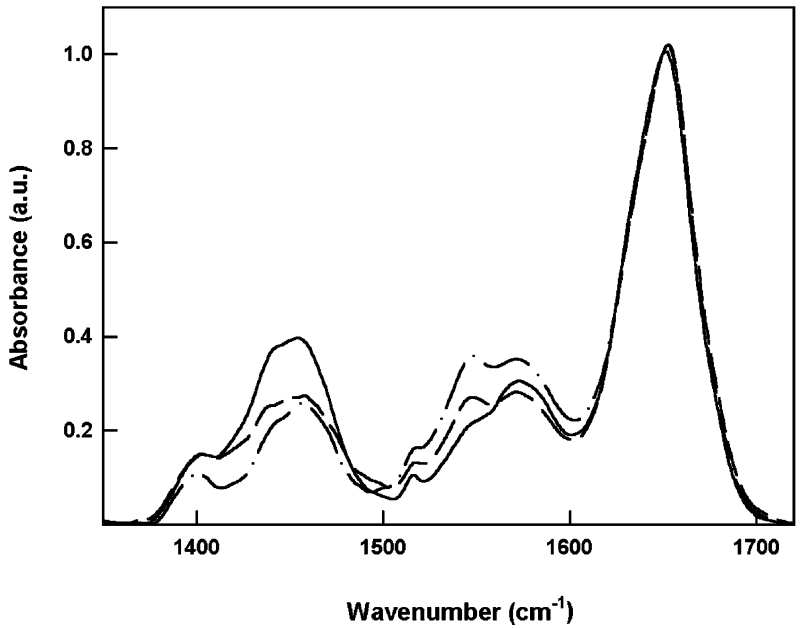

Fig. 4. Absorption spectra of BSA at room temperature in the Amides region. Solid line: pD 7.4; dashed line: pD 6.8; dashed–dotted line: pD 6.2.

conformation induced by pD, as also shown by the spectra at room temperature reported in Fig. 4. Once partial unfolding occurs, those differences found disappear. This behavior is to put in relation with the results obtained in a previous work, where we reported the steady-state fluorescence kinetic measurement of BSA and observed conformational changes at tertiary structure level at pH 6.2 within the first 100 min. Data shown in Figs. 3 and 4 suggest that, by lowering pD towards pI ($\sim$5 for this protein, [48]), the protein conformation appears more compact.

To follow the changes on secondary structure of BSA, we report in Fig. 5a the time evolution of IR spectra in the Amide I′ region. Fig. 5b shows the differential spectra obtained by subtracting to the spectrum at a generic time t, the initial spectrum at $t=0$. We can observe a progressive decrease of main contribution at 1650 cm^{-1} and the progressive increase of the two shoulders at 1620 and 1680 cm^{-1}, typically attributed to intermolecular β-sheet structures. The growth of these shoulders is correlated to the partial loss of the native α-helix secondary structure, as also put in evidence by the presence of two isosbestic points at 1630 and at 1670 cm^{-1}, suggesting a transition between these two secondary structures.

To see the role played by different pD values on the aggregation, we report in Fig. 6a the kinetic of IR spectra of BSA at pD 6.2 and in Fig. 6b the differential spectra of the same sample. A comparison of these data with those reported in Fig. 5 shows a substantial difference in the evolution of the spectra. At pD 6.2 the spectral contribution of the β-sheet aggregates at 1620 cm^{-1} appear with lower intensities and the shoulder at approximately 1680 cm^{-1} is not clear detectable; moreover, the overall Amide I′ band appears more asymmetrically broaden (Fig. 6b) as aggregation proceeds. Furthermore, the isosbestic points observed at pD 7.4 are not present, suggesting that the aggregation process is more complex than the simple α-helix $\rightarrow$ aggregated β-sheet transition. The increment of the width of Amide I′ band suggests an increase

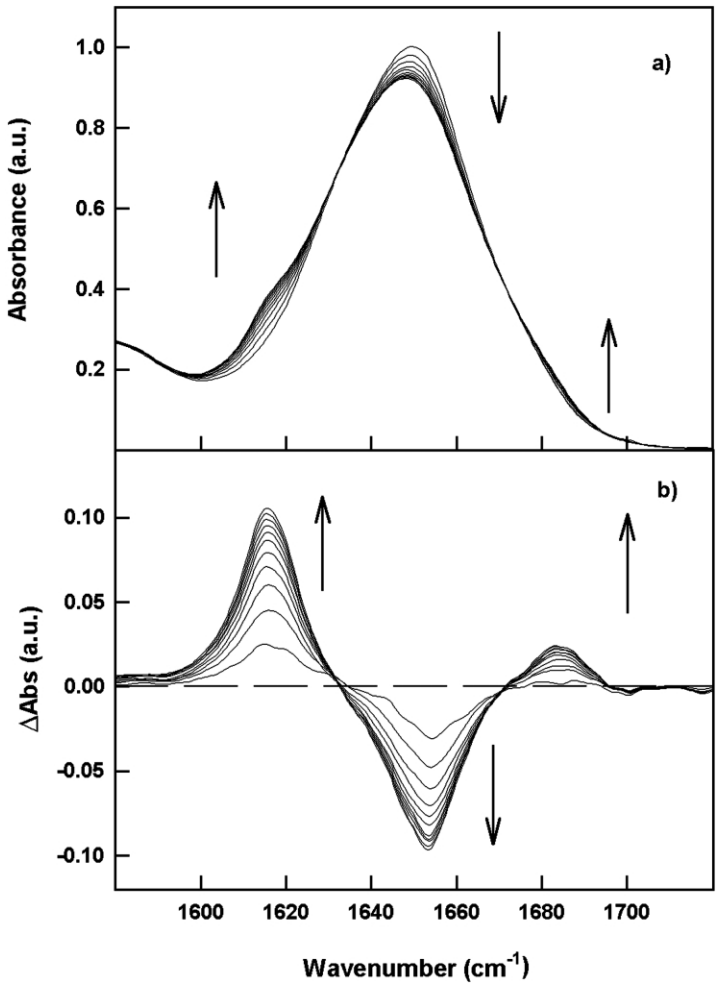

Fig. 5. Time evolution of Amide I′ spectral region of BSA, at pD 7.4 and at 58 °C: (a) absorption spectra; (b) differential spectra, defined as $\Delta A(t)=A(t)-A(t=0)$.

also in the random coil structures. An intermediate behavior is observed for kinetic measurements at pD 6.8 (data not reported).

To summarize the effects of pD on the spectral properties of BSA, we report in Fig. 7 the time evolution of the intensity of differential spectra at 1620 cm^{-1}. Data reported in Fig. 7 indicate that the amount of β-aggregates diminished when pD decreases.

To see if and how the above reported results on the structural changes induced by the temperature on BSA samples are related to the extent of the macromolecular aggregation process, we have performed light scattering measurements on the same samples. Fig. 8 shows the time evolution of the total scattered intensity at the three pD values, after suitable normalization. As can be seen, the growth of the aggregation is largely pD dependent; in particular, the extent of the aggregation increases by lowering pD.

A comparison between data in Figs. 7 and 8 put in evidence an apparent contradiction: in fact, if

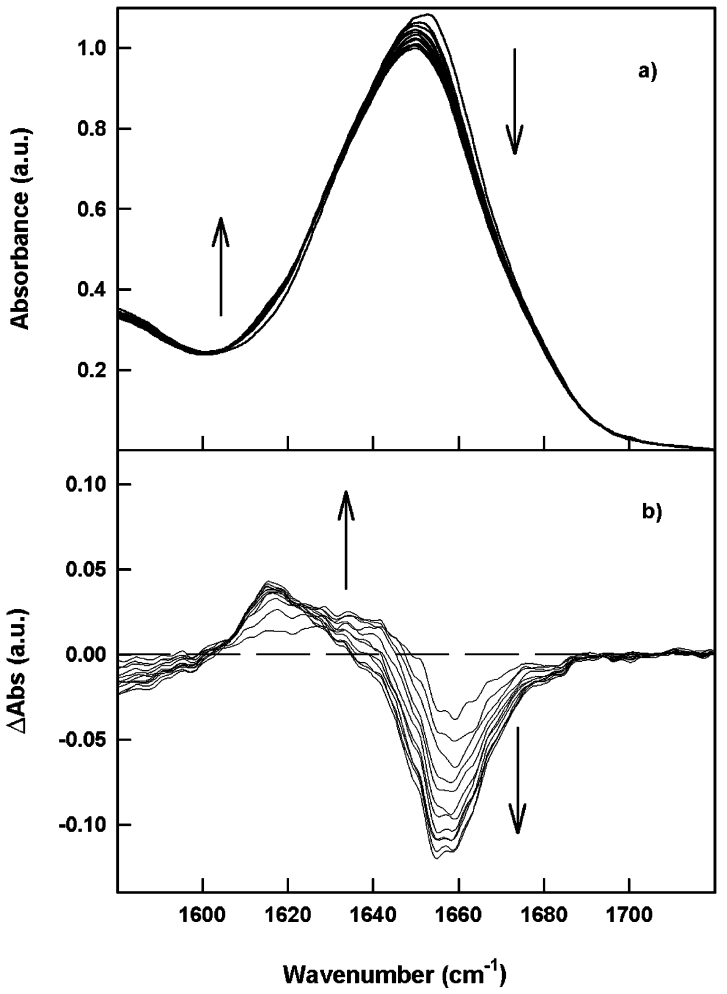

Fig. 6. Time evolution of Amide I′ spectral region of BSA, at pD 6.2 and at 58 °C: (a) absorption spectra; (b) differential spectra, defined as $\Delta A(t) = A(t) - A(t=0)$.

the formation of β-aggregates is the principal mechanism driving the process of macromolecular assembly, according to data in Fig. 7 we should have to expect that the extent of the aggregation will be smaller at low pD values, in contrast with data reported in Fig. 8. These considerations suggest that the aggregation mechanism is more complex and that other protein–protein interactions can contribute.

To have further information about this point, we have performed an analysis of the scattering data in terms of different contribution to the total intensity arising from different-in-size species, whose hydrodynamic radius can be determined. The results of this analysis is reported in Fig. 9 and compared with data obtained from IR measurements.

As can be seen from Fig. 9, left panels, at pD 7.4 the total intensity can be rationalized as the contribution of only one specie, whose hydrodynamic radius increases rapidly to a value of approximately 200 Å. This suggests that, at this pD value, the aggregation proceeds in a homogeneous way via formation of oligomers. To see if

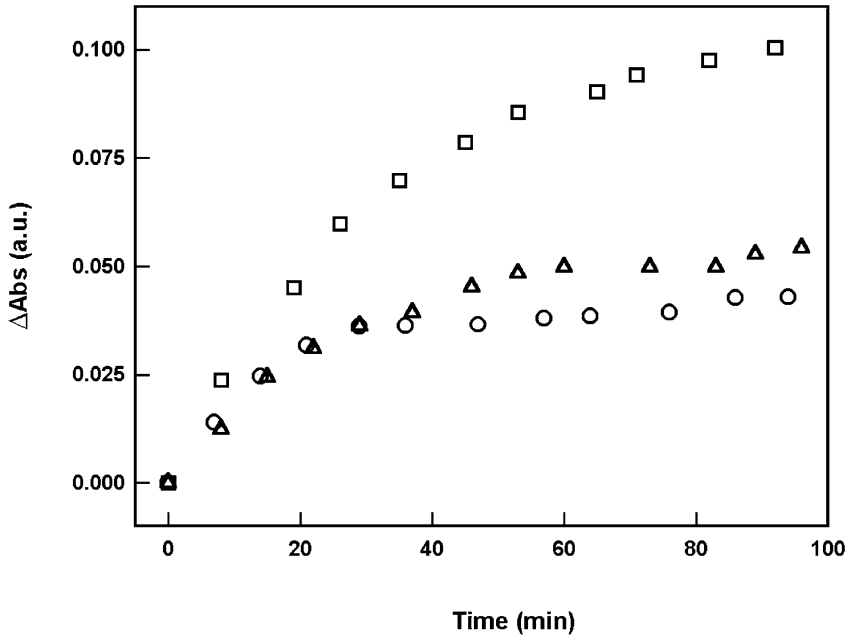

Fig. 7. Time evolution of the differential absorption intensity of Amide I′ component at 1620 cm^{-1} of BSA at 58 °C. Squares: pD 7.4; triangles: pD 6.8; circles: pD 6.2.

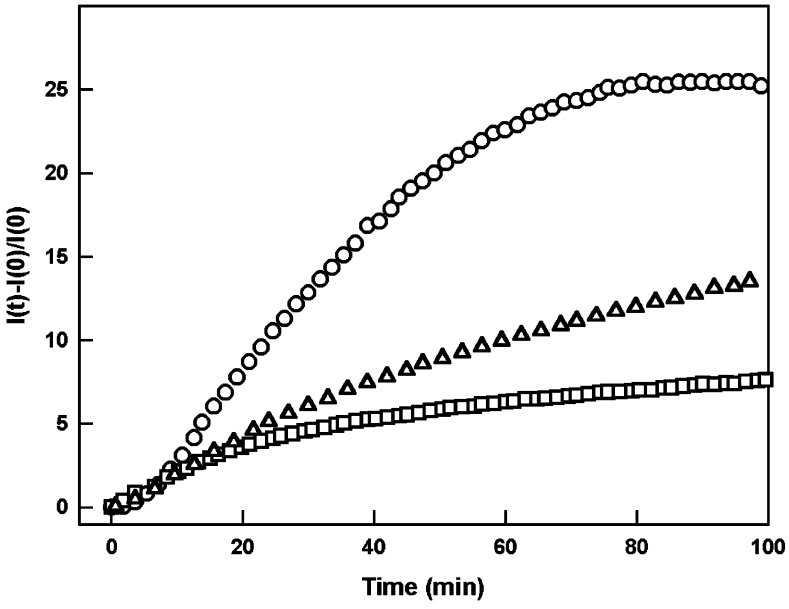

Fig. 8. Time evolution of the static light scattering intensity of BSA at 58 °C. Squares: pD 7.4; triangles: pD 6.8; circles: pD 6.2. Data are normalized for BSA concentration by dividing for initial scattering intensity of each sample, $I(0)$.

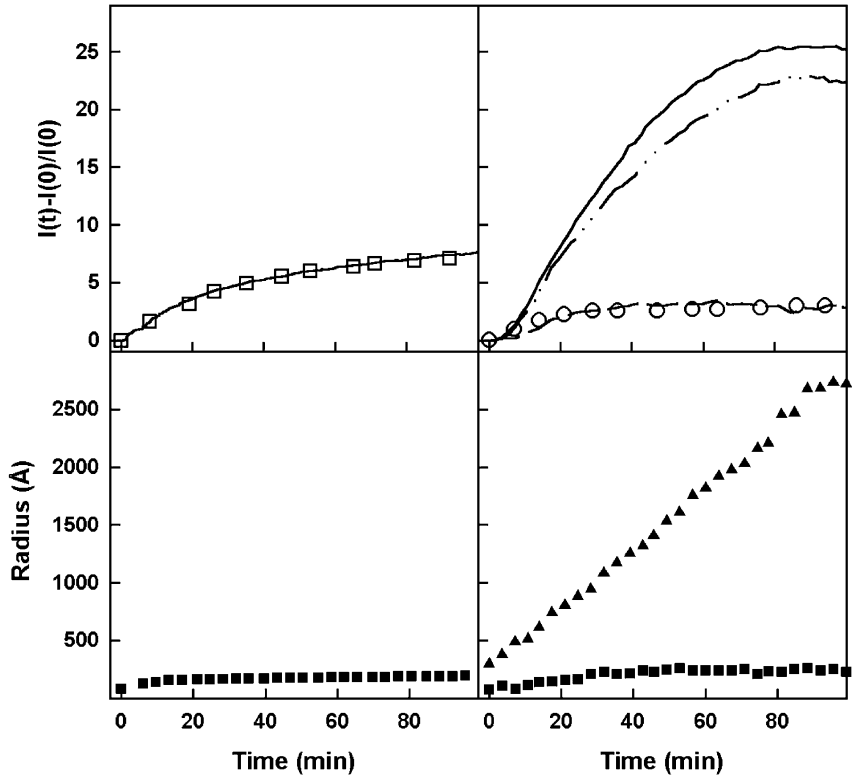

Fig. 9. *Top panels:* time evolution of total scattering intensity (solid lines) and of the contribution to the intensity of large (dashed–dotted lines) and small aggregates (dashed lines). *Bottom panels:* time dependence of the radii of large (triangles) and small (squares) aggregates; for the sake of clarity, not all the experimental points are reported. In the *upper panels* are also reported, for comparison, the time evolution of the intensity of Amide I′ component assigned to β-aggregates (open symbols), after suitable normalization (see text). *Left panels:* pD 7.4; *right panels*, pD 6.2.

the growth of β-aggregate structures is related to this mechanism, in the upper panels of Fig. 9 we have put on top the data relative to the total intensity of light scattering the differential IR intensity data, reported in Fig. 6, by a suitable scaling factor. As can be seen, IR data are almost coincident with light scattering ones, in the whole time interval studied, suggesting that, at this pD value, the aggregation proceeds essentially via β-aggregation. Different considerations must be made for data at lower pD values. As can be seen from Fig. 9, right panels, the total scattering intensity cannot be account by the contribution of only one specie. Data analysis shows the presence of two population distributions, one whose hydrodynamic radius do not exceeds the value of 150 Å (oligomers), and the other being characterized by very large radius, accounting for almost the 85% of the total intensity. IR data relative to the same sample are put on top of intensity scattering data, by the same scaling factor used for data at pD 7.4. As can be seen, IR data are almost coincident with the intensity contributions to total scattering due to the smaller specie (oligomers). Here we do not report the data at pD 6.8 that again show an intermediate behavior.

The fine analysis of the scattering data allows us to resolve the apparent contradiction above discussed. In fact, the decrease of the amount of β-aggregates (as the pD increases) is in favor of the appearance of other larger species that contribute to increase the total scattering intensity. From

all these results, the final considerations are that aggregation via β-aggregates is the mechanism that prevalently contributes to the oligomers formation, whereas other mechanisms add at lower pD values.

4. Conclusions

IR spectra and light scattering data of BSA show significant differences in terms of thermally induced aggregated structures at different pD values. The results are consistently in agreement and suggest that:

(i) At pD values far from the pI of the protein, i.e. when the net charge of the protein is increased, the aggregation mechanism proceeds in an ordered way to form β-aggregates that prevalently come from the α-helix changes and produce aggregates of small dimensions;

(ii) At pD values that approach the p*I*, i.e. when the net charge is decreased, the aggregation mechanism is more disordered and other aggregates of larger dimensions add to the smaller ones; moreover, a spectral disorder is also observed when the larger species appear, probably coming from increased amount of random coil structures;

(iii) Intra-molecular interactions change as a function of pD, i.e. the tertiary structures go towards partially unfolded conformations, as seen by Amide II spectral region, and are the first step towards the changes that drive to the aggregation, as also previously reported [27].

In other words, BSA can aggregates via smaller specie (β-aggregates) when the electrostatic repulsions are increased, this mechanism prevalently contributing to form oligomers, whereas other type of aggregates structures add when the net charge of the protein decreases. This behavior agrees with the results obtained by Clark et al. [5], that showed the formation of thermally induced ordered gels (in BSA and also in other proteins) at high pH, and of disorder gels at lower pH values, suggesting that the aggregation process becomes reminiscent of the precise molecular assembly mechanisms used by nature to achieve specific function (native structure). Moreover, the way in which the protein unfolds is clearly an important factor in determining the type of network formed and this is to put in correlation with the amount of tertiary and secondary structures lost during aggregation.

Acknowledgments

We wish to thank M.U. Palma and M.B. Palma-Vittorelli for useful discussions.

References

[1] G. Tabues, Misfolding the way to disease, Science 271 (1996) 1493–1495.
[2] M.F. Perutz, Mutations make enzyme polimeraze, Nature 385 (1997) 773–775.
[3] D.R. Booth, M. Sunde, V. Bellotti, et al., Instability, unfolding and aggregation of human lysozyme variants underlying amyloid fibrillogenesis, Nature 385 (1997) 787–793.
[4] F. Chiti, N. Taddei, F. Baroni, et al., Kinetic partitioning of protein folding and aggregation, Nat. Struct. Biol. 9 (2002) 137–143.
[5] A.H. Clark, F.J. Judge, J.M. Richards, J.M. Stubbs, A. Suggett, Electron microscopy of network structures in thermally-induced globular protein gels, Int. J. Pept. Prot. Res. 17 (1981) 380–392.
[6] A.H. Clark, G.M. Kavanagh, S.B. Ross-Murphy, Globular protein gelation—theory and experiment, Food Hydrocolloid. 15 (2001) 383–400.
[7] W. Wang, Instability, stabilization and formulation of liquid protein pharmaceuticals, Int. J. Pharm. 185 (1999) 129–188.
[8] C. Honda, H. Kamizono, T. Samejima, K. Endo, Studies on thermal aggregation of bovine serum albumin as a drug carrier, Chem. Pharm. Bull. 48 (2000) 464–466.
[9] J.H.M. Stokkum, H.L. Linsdell, J.M. Hadden, P.I. Haris, D. Chapman, M. Bloemendal, Temperature-induced changes in protein structures studied by Fourier transform infrared spectroscopy and global analysis, Biochemistry 34 (1995) 10508–10518.
[10] H.Y. Park, I.H. Song, J.-H. Kim, W.S. Kim, Preparation of thermally denatured albumin gel and its pH-sensitive swelling, Int. J. Pharm. 175 (1998) 231–236.
[11] G. Barone, C. Giancola, A. Verdoliva, DSC studies of the denaturation and aggregation of serum albumin, Thermochim. Acta 199 (1992) 197–205.
[12] E.L. Gelamo, M. Tabak, Spectroscopic studies on the interaction of bovine (BSA) and human (HSA) serum albumins with ionic surfactants, Spectrochim. Acta Part A 56 (2000) 2255–2271.
[13] T. Kosa, T. Maruyama, N. Otagiri, Species differences of serum albumins: II chemical and thermal stability, Pharm. Res. 15 (1998) 449–454.
[14] R. Jaenicke, Protein structure and function at low temperatures, Phylos. Trans. R. Soc. Lond. B 326 (1990) 535–551.

[15] F. Chiti, N.A.J. van Nuland, N. Taddei, et al., Conformational stability of muscle acylphosphatase: the role of the temperature, denaturant concentration and pH, Biochemistry 37 (1998) 1447–1455.
[16] Y. Goto, A.L. Fink, Acid-induced folding of heme proteins, Methods Enzymol. 232 (1994) 3–15.
[17] D.B. Volkin, A.R. Klibanov, Minimizing protein inactivation, in: T.E. Creighton (Ed.), Protein Function: A Practical Approach, Information Press, Oxford, UK, 1989, pp. 1–24.
[18] K.A. Dill, Dominant forces in protein folding, Biochemistry 29 (1990) 7133–7155.
[19] H.S. Chan, K.A. Dill, Polymer principles in protein structure and stability, Ann. Rev. Biophys. Chem. 20 (1991) 447–490.
[20] S.P.F.M. Roefs, K.G. De Kruif, A model for denaturation and aggregation of β-lactoglobulin, Eur. J. Biochem. 226 (1994) 883–889.
[21] P.L. San Biagio, D. Bulone, A. Emanuele, M.U. Palma, Self-assembly of biopolymeric structures below the threshold of random cross-link percolation, Biophys. J. 70 (1996) 494–499.
[22] P.L. San Biagio, V. Martorana, A. Emanuele, et al., Interacting processes in protein coagulation, Proteins: Struct. Funct. Gen. 37 (1999) 116–120.
[23] M. Bouchard, J. Zurdo, E.J. Nettleton, C.M. Dobson, C.V. Robinson, Formation of insulin amyloid fibrils followed by FTIR simultaneously with CD and electron microscopy, Protein Sci. 9 (2000) 1960–1967.
[24] Z. Szabó, K. Jost, K. Soós, M. Zarándi, J.T. Kiss, B. Penke, Solvent effect on aggregational properties of b-amyloid polypeptides studied by FT-IR spectroscopy, J. Mol. Struct. 480-481 (1999) 481–487.
[25] H.Y. Hu, Q. Li, H.C. Cheng, H.N. Du, β-Sheet structure formation of protein in solid state as revealed by circular dichroism spectroscopy, Biopolymers 62 (2001) 15–21.
[26] G.M. Kavanagh, A.H. Clark, S.B. Ross-Murphy, Heat-induced gelation of globular proteins. Part 3. Molecular studies on low pH β-lactoglobulin gels, Int. J. Biol. Macromol. 28 (2000) 41–50.
[27] V. Militello, V. Vetri, M. Leone, Conformational changes involved in thermal aggregation processes of bovine serum albumin, Biophys. Chem. 105 (2003) 133–141.
[28] A. Dong, J. Matsuura, S.D. Allison, E. Chrisman, M.C. Manning, J.F. Carpenter, Infrared and circular dichroism spectroscopic characterization of structural differences between β-lactoglobulin A and B, Biochemistry 35 (1996) 1450–1457.
[29] A. Dong, T.W. Randolph, J.F. Carpenter, Entrapping intermediates of thermal aggregation in α-helical proteins with low concentration of guanidine hydrochloride, J. Biol. Chem. 275 (2000) 27689–27693.
[30] H. Jiang, Z. Song, M. Lng, S. Yang, Z. Du, FTIR studies of recombinant human granulocyte-macrophage colony-stimulating factor in aqueous solution: secondary structure, disulfide reduction and thermal behaviour, Biochim. Biophys. Acta 1294 (1996) 121–128.
[31] F. Meersman, L. Smeller, K. Heremans, Comparative Fourier transform infrared spectroscopy study of cold-, pressure- and heat-induced unfolding and aggregation of myoglobin, Biophys. J. 82 (2002) 2635–2644.
[32] A.F. Allain, P.P. Paquin, M. Subirade, Relationships between conformation of β-lactoglobulin in solution and gel states as revealed by attenuated total reflection Fourier transform infrared spectroscopy, Int. J. Biol. Macromol. 26 (1999) 337–344.
[33] R.J. Green, I. Hopkinson, R.A.L. Jones, Unfolding and intermolecular association in globular proteins absorbed at interfaces, Langmuir 15 (1999) 5102–5110.
[34] J. Grdadolnik, Y. Maréchal, Bovine serum albumin observed by infrared spectrometry—I methodology, structural investigation, and water uptake, Biopolymers (Biospectrosc.) 62 (2001) 40–53.
[35] J. Grdadolnik, Y. Maréchal, Bovine serum albumin observed by infrared spectrometry—II hydration mechanism and interaction configurations of embedded H_2O molecules, Biopolymers (Biospectrosc.) 62 (2001) 54–67.
[36] F. Doesseau, M. Pezolet, Determination of the secondary structure content of protein in aqueous solutions from their Amide I and Amide II infrared bands. Comparison between classical and partial least-squares methods, Biochemistry 29 (1990) 8771–8779.
[37] A. Dong, P. Huang, W.S. Caughey, Redox-dependent changes in β-extended chain and turn structures of cytochrome *c* in water solution determined by second derivate Amide I infrared spectra, Biochemistry 31 (1992) 182–189.
[38] W.K. Surewicz, H.H. Mantsch, D. Chapman, Determination of protein secondary structure by Fourier transform infrared spectroscopy: a critical assessment, Biochemistry 32 (1993) 389–394.
[39] T.F. Kumosinski, J.J. Unruh, Quantitation of the global secondary structure of globular proteins by FTIR spectroscopy: comparison with X-ray crystallographic structure, Talanta 43 (1996) 199–219.
[40] A. Dong, P. Huang, W.S. Cauchey, Protein secondary structures in water from second-derivate amide I infrared spectra, Biochemistry 29 (1990) 3303–3308.
[41] D.M. Byler, H. Susi, Examination of the secondary structure of proteins by deconvolved FTIR Spectra, Biopolymers 25 (1986) 469–487.
[42] B.J. Berne, R. Pecora, Dynamic Light Scattering, Wiley, Chichester, New York, 1976.
[43] S.W. Provencher, A constrained regularization method for inverting data represented by linear algebraic or integral equations, Comput. Phys. Commun. 27 (1982) 213–227.
[44] D.E. Koppel, Analysis of macromolecular polydispersity in intensity correlation spectroscopy: the method of cumulants, J. Chem. Phys. 57 (1972) 4814–4820.

[45] E.L. Gelamo, C.H.T.P. Silva, H. Imasato, M. Tabak, Interaction of bovine (BSA) and human (HSA) serum albumins with ionic surfactants: spectroscopy and modeling, Biochim. Biophys. Acta 1594 (2002) 84–99.
[46] A.H. Clark, C.D. Tuffnel, Small-angle X ray scattering studies of thermally-induced globular protein gels, Int. J. Pept. Protein Res. 16 (1980) 339–351.
[47] A.H. Clark, D.H.P. Saunderson, A. Suggett, Infrared and laser-Raman spectroscopic studies of thermally-induced globular protein gels, Int. J. Pept. Protein Res. 17 (1981) 353–364.
[48] D.C. Carter, J.X. Ho, Structure of serum albumin, Adv. Protein Chem. 45 (1994) 153–203.